

FedZKT: Zero-Shot Knowledge Transfer towards Heterogeneous On-Device Models in Federated Learning

Lan Zhang, Xiaoyong Yuan

Michigan Technological University
{lanzhang, xyyuan}@mtu.edu

Abstract

Federated learning enables distributed devices to collaboratively learn a shared prediction model without centralizing on-device training data. Most of the current algorithms require comparable individual efforts to train on-device models with the same structure and size, impeding participation from resource-constrained devices. Given the widespread yet heterogeneous devices nowadays, this paper proposes a new framework supporting federated learning across heterogeneous on-device models via Zero-shot Knowledge Transfer, named by FedZKT. Specifically, FedZKT allows participating devices to independently determine their on-device models. To transfer knowledge across on-device models, FedZKT develops a zero-shot distillation approach contrary to certain prior research based on a public dataset or a pre-trained data generator. To utmostly reduce on-device workload, the resource-intensive distillation task is assigned to the server, which constructs a generator to adversarially train with the ensemble of the received heterogeneous on-device models. The distilled central knowledge will then be sent back in the form of the corresponding on-device model parameters, which can be easily absorbed at the device side. Experimental studies demonstrate the effectiveness and the robustness of FedZKT towards heterogeneous on-device models and challenging federated learning scenarios, such as non-iid data distribution and straggler effects.

1 Introduction

The demand for on-device training is recently increasing as evinced by the surging interest in federated learning (Yang et al. 2019). Federated learning leverages on-device training at multiple participating devices to obtain a knowledge-abundant global model without centralizing the private on-device data (McMahan et al. 2017; Li et al. 2019). Classical federated learning, represented by FedAvg (McMahan et al. 2017), requires learning on the same local model to perform the element-wise central average, which, however, impedes collaboration across *heterogeneous hardware platforms*. For instance, both wearable devices and smartphones are popular eHealth devices to monitor infectious diseases (Chen et al. 2021). However, a typical wearable device is usually equipped with the microcontroller units (MCU), whose on-chip memory is three orders of magnitude smaller than a smartphone due to the limited MCU resource budget, especially memory (SRAM) and storage (Flash) (Lin et al.

2020a). Hence, a wearable device can hardly run the same model designed for a smartphone (Cai et al. 2019), resulting in the ineffectiveness of classical federated learning.

Given the widespread yet heterogeneous devices in practice, a few recent efforts have been made on federated learning with heterogeneous on-device models. Diao *et al.* proposed HeteroFL to adaptively allocate subsets of global model parameters to on-device models (Diao, Ding, and Tarokh 2020). However, HeteroFL assumes the architecture of a small model can be a subnetwork of a large model, which is not always practical. For example, it is hard to find the architecture of MobileNet (Sandler et al. 2018), *i.e.*, a popular on-device model, as a subnetwork of other models, such as ShuffleNet (Ma et al. 2018) and ResNet (He et al. 2016). Instead, some recent research on federated distillation allows participating devices to independently design their on-device models. To transfer knowledge across heterogeneous models, logit information of on-device models is used in FedMD (Li and Wang 2019), Cronus (Chang et al. 2019), and FedH2L (Li et al. 2021b) for personalized, secure, and decentralized federated learning, respectively, while on-device model parameters are used in FedDF (Lin et al. 2020b) for robust model fusion. Although successful, all above algorithms are data-dependent, which leverage either a public dataset or a pre-trained data generator to extract on-device knowledge. Consequently, the construction of such data-dependency requires careful deliberation and even prior knowledge of the private on-device data, making it infeasible in many on-device applications. Moreover, the impact of the quality of such prerequisites remains unclear on federated learning performance.

To tackle the above limitations of prior research, in this paper, we propose a Zero-shot Knowledge Transfer framework named FedZKT for data-free federated learning across heterogeneous on-device models. Specifically, FedZKT allows participating devices to independently determine on-device models according to their resource capabilities in computation, communication, power, and storage. In addition, to utmostly reduce the on-device computational workload, FedZKT assigns the resource-intensive zero-shot knowledge distillation to the server, which constructs a generator to adversarially train with the ensemble of the received heterogeneous on-device models. The distilled central knowledge will then be sent back in the form of the cor-

responding on-device model parameters, which can be easily absorbed at the device side. In other words, FedZKT enables broad participation, especially for resource-constrained devices, to locally train and upload compact models with a reduced on-device computational and communication cost. Overall, FedZKT consolidates several *advantages* into a single framework: independent on-device model design, participation from resource-constrained devices, and data-free knowledge transfer. Our main contributions are as follows:

- This paper introduces a new federated learning framework named by FedZKT to perform zero-shot knowledge transfer across heterogeneous on-device models. Several key components are identified to enable lightweight and resource-intensive computation respectively at the device side and the server side, which perfectly fit the fact of unbalanced resources on both sides.
- Contrary to certain prior research based on either a public dataset or a pre-trained data generator, FedZKT provides a zero-shot solution without data-dependency concerns, where the server adversarially learns a generative model with the global model based on the ensemble of the received heterogeneous on-device models.
- Experimental studies demonstrate the effectiveness of FedZKT on MNIST, KMNIST, FASHION-MNIST, and CIFAR-10 datasets with higher accuracy and better generalization performance, compared with the state-of-the-art. FedZKT also performs robustness to challenging federated learning scenarios, such as non-iid data distribution and straggler effects.

2 Related Work

Federated Learning. Classical federated learning, such as FedAvg (McMahan et al. 2017), averages the received on-device model parameters to obtain a global model. Since the training mainly happens locally, the overall training performance largely depends on each participating device. It has been shown that statistical heterogeneity, *i.e.*, non-iid local data, can lead to slow and unstable convergence (Li et al. 2019). Such performance degradation has also been found when on-device resources (*e.g.*, computational power and network connectivity) are heterogeneous (Li et al. 2020). Although recent research has developed solutions to either address the “straggler effect” due to some poorly performed devices (Liu et al. 2020; McMahan et al. 2017; Li et al. 2020; Nishio and Yonetani 2019) or reduce the local model size at all devices (Vepakomma et al. 2018; He, Annavaram, and Avestimehr 2020), they are still under the training paradigm of FedAvg, *i.e.*, all devices need to run the on-device models with the same structure and size.

Federated Distillation. Knowledge distillation has been a well-known technique to transfer knowledge from a single or multiple teacher models to an empty student model (Buciluă, Caruana, and Niculescu-Mizil 2006; Ba and Caruana 2013; Hinton, Vinyals, and Dean 2015). Typically, the same dataset is shared between teacher and student, where the outputs of teacher models are used to train the student. Enlighten by this, federated distillation learns a global

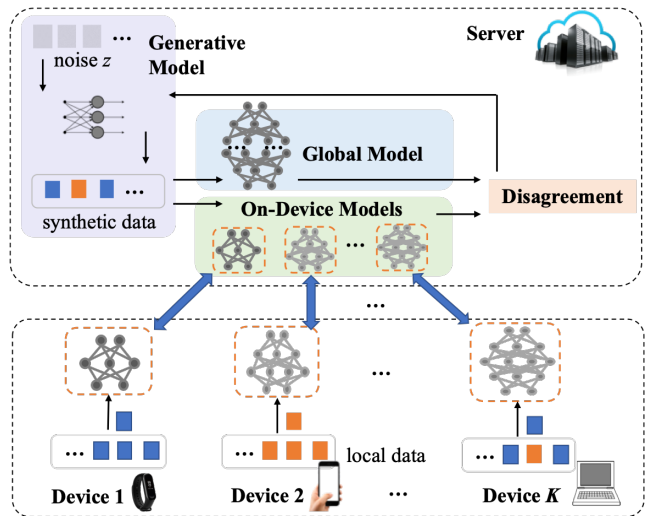


Figure 1: **Overview of FedZKT: Zero-shot knowledge transfer for federated learning across heterogeneous on-device models.** Most workloads of FedZKT are completed at the server side. Participating devices only need to train the on-device models on their local data.

model based on on-device models, which recently attracts great attention. Most federated distillation research is data-dependent by leveraging a public or surrogate dataset to improve or handle communication efficiency (Jeong et al. 2018; Guha, Talwalkar, and Smith 2019; Itahara et al. 2020; Sattler et al. 2020; Seo et al. 2020), on-device privacy (Sun and Lyu 2020; Chang et al. 2019), data heterogeneity (Chen and Chao 2020; Sattler et al. 2021), and the aforementioned model heterogeneity (Li and Wang 2019; Chang et al. 2019; Lin et al. 2020b; Li et al. 2021b). However, the prerequisite of the data-dependency is not always available for knowledge distillation due to the unknown or confidential data distribution of teacher models. Moreover, the absence of a qualified public or surrogate dataset will return a poor approximation of teacher models (Truong et al. 2021).

Data-Free Knowledge Distillation. To tackle the above data dependency prerequisite in knowledge distillation, zero-shot (data-free) knowledge distillation has been proposed to train a generative model to synthesize the queries that the student makes to the teacher (Fang et al. 2019; Miccaelli and Storkey 2019; Choi et al. 2020; Truong et al. 2021). (Zhu, Hong, and Zhou 2021) implemented the data-free techniques in FeDGen to handle data heterogeneity in federated learning, where the generator is iteratively broadcasted from the server to all devices to locally augment the on-device knowledge. Instead, in this paper, the server keeps the generator to process the data-free distillation, and returns the augmented on-device knowledge to utmostly reduce on-device workload, which enables a broad participation especially from resource-constrained devices as shown in Figure. 1.

Algorithm 1: FedZKT

INPUT: global model parameters w , on-device model parameters $\{w_k\}_{k \in \mathcal{K}}$, generative model parameters θ , total communication rounds T , local training epochs T_l , distillation epochs n_D .

```
1: Initialize all models with random weights1.
2: for each communication round  $t = 1, 2, \dots, T$  do
3:    $\mathcal{K}^t \leftarrow$  server selects a random subset devices from  $\mathcal{K}$  as active devices
4:   // On-Device Update
5:   for each device  $k \in \mathcal{K}^t$  in parallel do
6:      $\hat{w}_k \leftarrow$  OnDeviceUpdate( $w_k, \mathcal{D}_k, T_l, n_D$ )
7:     Upload  $\hat{w}_k$  to the server.
8:   end for
9:   // Server Update
10:   $\{w_k\}_{k \in \mathcal{K}}, w, \theta \leftarrow$  ServerUpdate( $\{\hat{w}_k\}_{k \in \mathcal{K}}, w, \theta$ ).
11:  for each device  $k \in \mathcal{K}$  in parallel do
12:    Transfer  $w_k$  to Device  $k$ .
13:  end for
14: end for
RETURN:  $w, \{w_k\}_{k \in \mathcal{K}}$ 
```

3 FedZKT: Federated learning via Zero-shot Knowledge Transfer

This section presents the proposed FedZKT. We first introduce the problem statement, followed by the algorithm design, and finally detail several key modules of FedZKT at both the server and device sides.

3.1 Problem Statement

As shown in Figure 1, we consider a federated learning task, e.g., a supervised classification task, across K devices in set \mathcal{K} . Each device $k \in \mathcal{K}$ independently designs its local model f_k parameterized by w_k to “best” fit its own resources in computation, communication, storage, and power. Thus, the on-device models $\{f_k\}_{k \in \mathcal{K}}$ may have distinct model architectures. In addition, we assume each device owns a confidential dataset \mathcal{D}_k , and thus the server has no prior knowledge about the data distribution at the device side. The server is assumed to be powerful, who will coordinate all devices to aggregate their on-device knowledge. The main goal of the server is to extract the distributed on-device knowledge from the heterogeneous on-device models $f_{k \in \mathcal{K}}$ to obtain a knowledge-abundant global model F , while providing updated on-device models $f_{k \in \mathcal{K}}$ that contain the distilled knowledge from other peer devices.

3.2 FedZKT Algorithm

To meet the unbalanced computational capabilities between the server and devices (e.g., IoT devices), FedZKT assigns the resource-intensive knowledge distillation task to the server. We elaborate the algorithm procedures of FedZKT in Algorithm 1, and describe the design principle of several key modules below.

Algorithm 2: FedZKT: OnDeviceUpdate

INPUT: on-device model f_k 's parameters w_k , local dataset \mathcal{D}_k , local epochs T_l

```
1: for  $t \in \{1, 2, \dots, T_l\}$  do
2:    $\mathcal{L}_k \leftarrow \sum_{\{x, y\} \in \mathcal{D}_k} \mathcal{L}_{CE}(f_k(x; w_k), y)$ 
3:    $w_k \leftarrow w_k - \eta \frac{\partial \mathcal{L}_k}{\partial w_k}$ 
4: end for
RETURN:  $w_k$ 
```

Algorithm 3: FedZKT: ServerUpdate

INPUT: global model \mathcal{F} 's parameters w , on-device model f_k 's parameters $\{w_k\}_{k \in \mathcal{K}}$, generator G 's parameters θ , distillation epochs n_D .

```
1: // Transfer knowledge from on-device models to the global model
2: for  $n \in \{1, 2, \dots, n_D\}$  do
3:   // Generator Update
4:    $z \sim \mathcal{N}(0, \mathbf{I})$ 
5:    $x \leftarrow G(z; \theta)$ 
6:    $\mathcal{L}_G \leftarrow -\mathcal{L}(\mathcal{F}(x; w), \frac{1}{|\mathcal{K}|} \sum_{k \in \mathcal{K}} f_k(x; w_k))$ 
7:    $\theta \leftarrow \theta - \eta_G \frac{\partial \mathcal{L}_G}{\partial \theta}$ 
8:   // Global Model Update
9:    $z \sim \mathcal{N}(0, \mathbf{I})$ 
10:   $x \leftarrow G(z; \theta)$ 
11:   $\mathcal{L}_S \leftarrow \mathcal{L}(\mathcal{F}(x; w), \frac{1}{|\mathcal{K}|} \sum_{k \in \mathcal{K}} f_k(x; w_k))$ 
12:   $w \leftarrow w - \eta_S \frac{\partial \mathcal{L}_S}{\partial w}$ 
13: end for
14: // Transfer knowledge from the global model to on-device models
15: for  $n \in \{1, 2, \dots, n_D\}$  do
16:    $z \sim \mathcal{N}(0, \mathbf{I})$ 
17:    $x \leftarrow G(z; \theta)$ 
18:   for each device  $k \in \mathcal{K}$  do
19:      $\mathcal{L}_k \leftarrow \mathcal{L}(\mathcal{F}(x; w), f_k(x; w_k))$ 
20:      $w_k \leftarrow w_k - \eta_S \frac{\partial \mathcal{L}_k}{\partial w_k}$ 
21:   end for
22: end for
RETURN:  $\{w_k\}_{k \in \mathcal{K}}, w, \theta$ 
```

Zero-Shot Knowledge Distillation. The goal of our knowledge distillation is to train the global model $\mathcal{F}(\cdot; w)$ to match the ensemble of on-device models $\{f_k\}_{k \in \mathcal{K}}$ that are trained on private local knowledge domain $\mathcal{D}_{k \in \mathcal{K}}$. Due to the unavailability of $\mathcal{D}_{k \in \mathcal{K}}$, a synthetic dataset \mathcal{D}_S is used to minimize the loss of disagreement between the teacher and the students using ensemble learning,

$$\min_w E_{x \sim \mathcal{D}_S} [\mathcal{L}(\mathcal{F}(x; w), f_{\text{ens}}(G(z)))], \quad (1)$$

where f_{ens} denotes the ensemble of the on-device models, i.e., $f_{\text{ens}} = \frac{1}{|\mathcal{K}|} \sum_k f_k(x)$. \mathcal{L} denotes the loss function to measure the disagreement between two models that will

¹This work uses Glorot initialization (Glorot and Bengio 2010). The same initialization is not required for on-device models.

be detailed in Section 3.2. To derive \mathcal{D}_S to synthesize local knowledge domain, a generative model G is introduced for zero-shot distillation upon the well-known idea of Generative Adversarial Networks (GAN) (Truong et al. 2021). Specifically, G is responsible to provide difficult input for the training of \mathcal{F} , which maximizes the disagreement between the current global and local models, while the generated input data is expected to perform well in (1) to enable knowledge matching between the global and local models. Hence, G and \mathcal{F} aim to maximize and minimize the disagreement between \mathcal{F} and $f_{k \in \mathcal{K}}$, respectively. The adversarial game can be given by

$$\min_{\mathcal{F}} \max_G E_{z \sim \mathcal{N}(0,1)} [\mathcal{L}(\mathcal{F}(G(z)), f_{\text{ens}}(G(z)))]. \quad (2)$$

Therefore, the server will alternatively train the generative model G and global model \mathcal{F} in (2). It should be mentioned most prior knowledge distillation performs well when extracting a small student model from a large teacher, while some recent research (Micaelli and Storkey 2019; Truong et al. 2021) has shown high accuracy even when a teacher model’s architecture is smaller and different than that of a student. Hence, this work is further motivated to extract a knowledge-abundant global model from heterogeneous and potentially compact on-device models using ensemble learning.

Bidirectional Knowledge Transfer. The above module transfers knowledge from participating devices to the server. After that, the aggregated server knowledge needs to transfer back to devices for the next learning iteration. One intuitive approach is to broadcast the updated global model \mathcal{F} , based on which, each device can use its own data to distill an updated on-device model, similar to the above module based on (1). However, this paper aims to enable federated learning with heterogeneous devices, which allows broad participation from resource-constrained devices. Thus, to utmostly reduce the on-device workload, we run knowledge distillation from \mathcal{F} to $f'_{k \in \mathcal{K}}$ at the server. Since the above module learns the G to generate difficult data that maximizes the disagreement between global and on-device models, we reuse this G to provide input data to distill the updated on-device model $f'_{k \in \mathcal{K}}$. Hence, the objective function for knowledge transfer from \mathcal{F} to f_k for all $k \in \mathcal{K}$ is given by

$$\min_{f_k} E_{z \sim \mathcal{N}(0,1)} [\mathcal{L}(\mathcal{F}(G(z)), f_k(G(z)))]. \quad (3)$$

The updated on-device model f'_k will be sent back to device k , which completes one-round bidirectional knowledge transfer. Since the computation for (2) and (3) is performed at the server, FedZKT does not increase on-device workload.

Loss Function of Knowledge Distillation. The loss function \mathcal{L} in (2) measures the model disagreement, which is used to train the global model and generative model. Most of prior knowledge distillation measures model disagreement by KL-divergence loss. By applying KL-divergence loss in Algorithm 1, the loss function can be written as

$$\mathcal{L}_{\text{KL}}(x) = \sum \mathcal{F}(x) \log \frac{\mathcal{F}(x)}{f_{\text{ens}}(x)}, \quad (4)$$

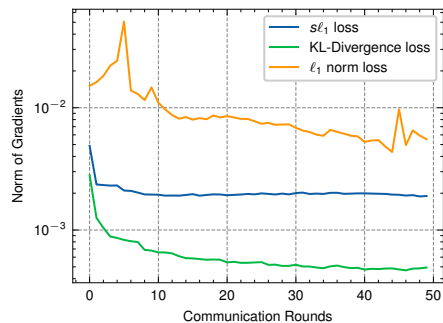


Figure 2: **Norm of gradients w.r.t input data (MNIST, IID).** The gradients for KL divergence loss tend to vanish, while the gradients for ℓ_1 norm loss are much larger and unstable during the learning process. The proposed SL loss overcomes both problems in the federated learning.

where $\mathcal{F}(x)$ and $f_{\text{ens}}(x)$ denote the outputs of the global model and the ensemble of on-device models after the softmax function, respectively. However, KL-divergence loss may lead to gradient vanishing with respect to the input data x when the student model converges to the teacher model, which affects the training of the generative model. Therefore, recent zero-shot knowledge distillation (Fang et al. 2019; Truong et al. 2021) uses ℓ_1 norm loss in knowledge distillation, which compares the logit outputs (model outputs before the softmax layer) between models:

$$\mathcal{L}_{\ell_1}(x) = \|u(x) - \frac{1}{|\mathcal{K}|} \sum_k v_k(x)\|_1, \quad (5)$$

where u and v_k denote the logit outputs of the global and on-device models, respectively. However, given the diverse model parameters of on-device models, ℓ_1 norm loss may lead to unstable training due to the large gradients. Specifically, federated learning requires aggregating knowledge from participating devices, but averaging the logit values over on-device models increases the gradients, making the learning process unstable. Therefore, we introduce a new loss function, SL loss, which applies the softmax output to the ℓ_1 loss:

$$\mathcal{L}_{\text{SL}}(x) = \|\mathcal{F}(x) - f_{\text{ens}}(x)\|_1, \quad (6)$$

which overcomes the drawback of using KL-divergence and ℓ_1 norm losses for zero-shot knowledge distillation in federated learning. We describe Hypothesis 1 and 2 below, which shows the above observation. More details are provided in the Appendix. The empirical evaluation is given in Section 4.3. Figure 2 shows the norm of gradients for KL divergence, ℓ_1 norm, and the proposed SL norm losses.

Hypothesis 1. *When the global model F converges to the ensemble of on-device models f_{ens} , the gradients of KL divergence loss with respect to the input data x are smaller than those of the SL loss:*

$$\|\nabla_x \mathcal{L}_{\text{KL}}(x)\|_{F \rightarrow f_{\text{ens}}} \leq \|\nabla_x \mathcal{L}_{\text{SL}}(x)\|. \quad (7)$$

Hypothesis 2. When the global model F converges to the ensemble of on-device models f_{ens} , the gradients of the ℓ_1 norm loss with respect to the input data x are greater than those of the SL loss:

$$\|\nabla_x \mathcal{L}_{\ell_1}(x)\|_{F \rightarrow f_{\text{ens}}} \geq \|\nabla_x \mathcal{L}_{\text{SL}}(x)\|. \quad (8)$$

ℓ_2 Regularization for Non-IID Data Distribution. In addition to tackle the model architecture heterogeneity, FedZKT addresses the challenges the variability of data distributions in federated learning. We limit the update of on-device models when training the on-device models on the local datasets. We add a ℓ_2 regularization to the loss function of the on-device update (Algorithm 2):

$$\min_{w_k^t} \sum_{\{x,y\} \in \mathcal{D}_k} \mathcal{L}_{CE}(f_k(x; w_k^t), y) + \|w_k^t - w_k^{t-1}\|_2^2, \quad (9)$$

where \mathcal{L}_{CE} is the cross-entropy loss in the classification tasks and w_k^{t-1} is the parameter transferred from the server. FedProx (Li et al. 2018) uses ℓ_2 regularization to tackle the non-iid data distribution with homogeneous model architectures and improves the stability of the learning process. By introducing ℓ_2 regularization, we tackle both data and model heterogeneity. Compared with FedProx, due to model heterogeneity, we have to use the transferred local parameters w_k^{t-1} rather than the global model weights w^{t-1} in FedZKT. The empirical evaluation demonstrates the improvement of adding ℓ_2 regularization for non-iid data distributions (Section 4.3).

4 Experiments

This section evaluates the proposed FedZKT on various heterogeneous federated learning settings. More implementation details and extended experimental results can be found in the Appendix.

4.1 Experimental Setup

Datasets. We conduct experiments on four widely used image datasets: MNIST (LeCun et al. 1998), KMNIST (Clanuwat et al. 2018), FASHION-MNIST (Xiao, Rasul, and Vollgraf 2017) (FASHION in short in this paper), and CIFAR-10 (Krizhevsky et al. 2009).

Model Heterogeneity. We conduct experiments on ten devices in federated learning. We use five different neural network architectures for each dataset and deploy the ten devices’ on-device models with the five neural architectures. For the small datasets, we deploy a CNN model, a Fully-Connected Model, and three LeNet-like models with different channel sizes and numbers of layers. For the CIFAR-10 dataset, we deploy two ShuffleNetV2 models (Ma et al. 2018), two MobileNetV2 models (Sandler et al. 2018), and a LeNet-like model. ShuffleNetV2 and MobileNetV2 are popular neural architectures that are designed towards low-end devices. LeNet is a simple neural network architecture consisting of two convolutional layers and three fully connected layers. We use different channel sizes for each ShuffleNetV2

and MobileNetV2 model, so as to increase the heterogeneity of models in the evaluation. We describe the details of all the model architectures and architecture assignment in Appendix.

Federated Learning Settings. For small datasets (e.g., MNIST, KMNIST, FASHION), we run 50 communication rounds ($T = 50$), and in each round, each device trains local models for 5 epochs. For the CIFAR-10 dataset, we run 100 communication rounds ($T = 100$) and in each round, each device trains on-device models for 10 epochs. We use SGD to train on-device models and the server model set with a learning rate of 0.01. We train the server model and generator for 200 iterations for the small datasets ($n_G = n_s = 200$) and 500 iterations for the CIFAR-10 dataset ($n_G = n_s = 500$). The generator is trained using Adam optimizer with a batch size of 256 and a learning rate of 0.001. We apply learning rate decay for both the server model and generator. The learning rate will be reduced by 0.3 at We set the batch size for all model training as 256.

Data Heterogeneity. We evaluate the proposed FedZKT on both iid and non-iid data distributions. In the iid data setting, each device’s private data is randomly drawn from the dataset. In the non-iid data setting, we consider two scenarios of label distribution skew, following the common experimental settings in recent non-iid federated learning works (Wang et al. 2020; Li et al. 2021a): 1) Quantity-based label imbalance, where each device owns data consisting of a specific number of classes. 2) Distribution-based label imbalance, where each device owns a proportion of the labels following a Dirichlet distribution. We sample $p_k = \{p_{kj}\}$ from $Dir_N(\beta)$, where p_{kj} denotes the proportion of data of class k owned by device j and β is a concentration parameter of the Dirichlet distribution. A small value of β suggests a more imbalanced distribution of labels.

Baseline Approach. As aforementioned, all existing federated learning for heterogeneous on-device models is data-dependent, based on a public dataset or a pre-trained generator. We adopt the most representative algorithm, FedMD (Li and Wang 2019) as the baseline approach for the proposed data-free FedZKT. Similar to FedZKT, FedMD allows devices to independently design on-device models, which provides extensive experimental results for on-device model heterogeneity but requiring a public dataset. To learn from MNIST, FASHION, and KMNIST, we select public datasets as FASHION, MNIST, and FASHION, respectively. To explore the impact of data dependency in knowledge transfer, we select two different public datasets (CIFAR-100 and SVHN) to learn CIFAR-10.

4.2 Experimental Results

IID data distribution. We report the average accuracy of ten devices using FedMD and FedZKT. From Table 1, we observe that, overall, FedZKT achieves higher accuracy than FedMD. More importantly, the performance of FedMD relies on the similarity of data distribution between the public dataset and private on-device datasets. FedMD uses two different public datasets (CIFAR-100 and SVHN) to train on

| Dataset | FedMD | | FedZKT |
|----------|----------------|------------------|------------------|
| | Public dataset | Average accuracy | Average accuracy |
| MNIST | FASHION | 96.69% | 97.76% |
| FASHION | MNIST | 85.83% | 84.42% |
| KMNIST | FASHION | 84.02% | 86.43% |
| CIFAR-10 | CIFAR-100 | 67.34% | 78.02% |
| CIFAR-10 | SVHN | 20.38% | |

Table 1: IID performance of FedZKT and FedMD.

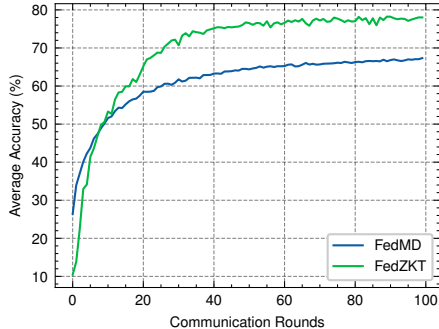


Figure 3: **Learning curves of FedZKT and FedMD (CIFAR-10, IID).**

the CIFAR-10 dataset. We observe that FedMD achieves a higher accuracy on the CIFAR-10 dataset when the server could use a similar dataset (CIFAR-100). However, when the data distribution of the public dataset (SVHN) is different from that of on-device datasets, the performance of FedMD drops significantly. Hence, it is critical but extremely challenging for FedMD to select a proper public dataset since the server may have no access to the private on-device dataset.

Figure 3 shows the learning curves of FedZKT and FedMD on the CIFAR-10 dataset with IID data distribution. FedMD uses the CIFAR-100 dataset as the public dataset to assist federated learning. Since the public dataset here is close to the data distribution of the private on-device dataset, FedMD learns the task better than FedZKT at the beginning of training. However, with the learning process, FedZKT learns from the local data and improves the generator through knowledge transferring; meanwhile, FedMD can only use the data from the public dataset, which cannot be improved during learning. Thus, FedZKT eventually outperforms FedMD.

Non-IID data distribution. We evaluate the performance of FedZKT in non-iid data distribution. We use four values of the number of classes owned by each device $c \in \{2, 3, 4, 5\}$ for the quantity-based label imbalance scenario, and four values of the concentration parameter $\beta \in \{0.1, 0.5, 1, 5\}$ for the distribution-based label imbalance scenario. We compare FedZKT with FedMD in both scenarios. As shown in Figure 4 and 5, FedZKT is more robust compared to FedMD in almost all non-iid data distribution.

| Non-IID scenario | KL divergence | ℓ_1 norm | SL loss |
|------------------|---------------|---------------|---------------|
| $C = 5$ | 48.23% | 14.60% | 63.89% |
| $\beta = 0.5$ | 66.17% | 16.34% | 69.39% |

Table 2: Comparison of loss functions (CIFAR-10).

| Non-IID scenario | Without regularization | ℓ_2 regularization |
|------------------|------------------------|-------------------------|
| $C = 5$ | 56.58% | 63.89% |
| $\beta = 0.5$ | 66.17% | 69.39% |

Table 3: Effect of ℓ_2 regularization in FedZKT (CIFAR-10).

4.3 Ablation Studies

We perform the ablation studies below to evaluate the impact of key components (modules) in FedZKT.

Choice of Loss Function in FedZKT. We evaluate the performance of different loss functions used in FedZKT in terms of two non-iid scenarios: 1) distribution-based label imbalance with $\beta = 0.5$ and quantity-based label imbalance with $c = 5$. As shown in Table 2, the proposed SL loss achieves better performance than KL Divergence and ℓ_1 loss on both scenarios. Although ℓ_1 norm avoids gradient vanishing in zero-shot knowledge distillation, ℓ_1 norm causes unstable training in federated learning, especially in the non-iid scenarios.

Effects of ℓ_2 Regularization. We evaluate the performance of the ℓ_2 regularization in FedZKT. As shown in Table 3, the performance of using ℓ_2 regularization is better than that ℓ_2 without the ℓ_2 regularization in non-iid scenarios of both distribution-based label imbalance and quantity-based label imbalance, which demonstrates the effectiveness of the ℓ_2 regularization.

Effects of Model Architectures. Figure 6 shows the devices’ learning curves of FedZKT. The performance of each device’s learning curves relies on the capabilities of the model architectures. Device 5 and Device 10 use a simple LeNet-like neural network. Due to its simple model architecture, the performance of the LeNet-like model is lower than that of the ShuffleNetV2 and MobileNetV2 models. We report the performance of each model architecture in the Appendix. The proposed FedZKT is very close to the upper-bound performance of each model architecture, *i.e.*, when the model is trained on the combination of all local datasets.

Effects of Device Number. We evaluate the effect of different numbers of devices ($K \in \{5, 10, 15, 20\}$) on FedZKT. As shown in Figure 7, the number of devices does not affect the training of FedZKT too much. A smaller number of devices (*e.g.*, $K = 5$) may achieve higher average accuracy, but FedZKT can achieve good performance with more devices as well. As observed from experiments, the effect of different numbers of devices is subtle (around $\pm 2\%$ in terms of average accuracy).

Effects of Stragglers. Federated learning may suffer from the straggler effects, where a subset of devices cannot participate in training in some rounds due to their unstable network communication, low battery conditions, etc. To eval-

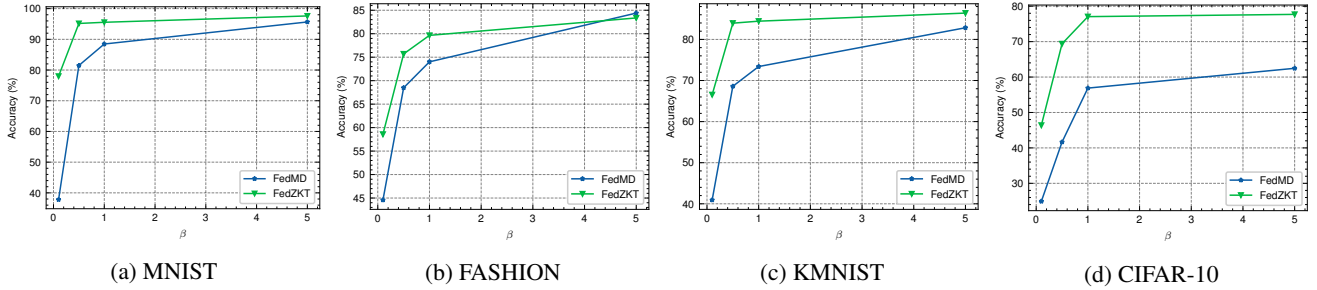


Figure 4: Non-IID performance of FedZKT and FedMD (distribution-based label imbalance).

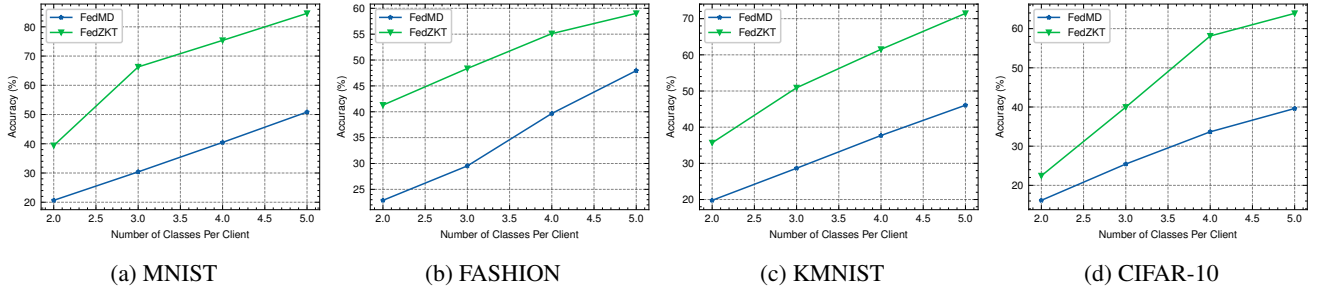


Figure 5: Non-IID performance of FedZKT and FedMD (quantity-based label imbalance).

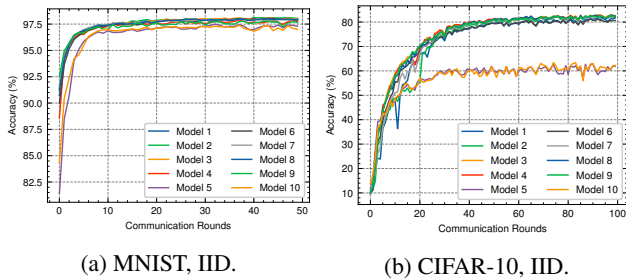


Figure 6: Learning Curves of On-Device Models.

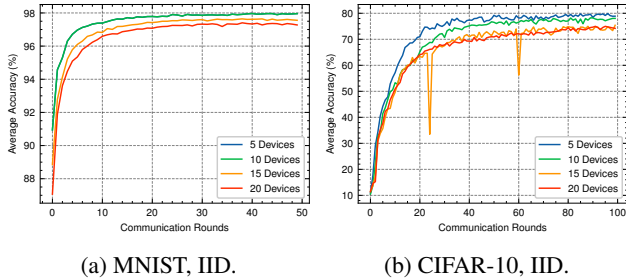


Figure 7: Effects of device number. The figures show the average accuracies of K on-devices models participated in federated learning ($K \in \{5, 10, 15, 20\}$).

uate the effect of stragglers in FedZKT, in each communication round, we randomly select a portion of devices ($p \in \{0.2, 0.4, 0.6, 0.8, 1.0\}$) as active devices who participate in federated learning. The rest devices (inactive devices) are unable to contribute to federated learning. To evaluate the performance of FedZKT, we follow the same procedure in Algorithm 1 and do not update the parameters for inactive devices. As shown in Figure 8, the performance of FedZKT is degraded only when a very small portion of de-

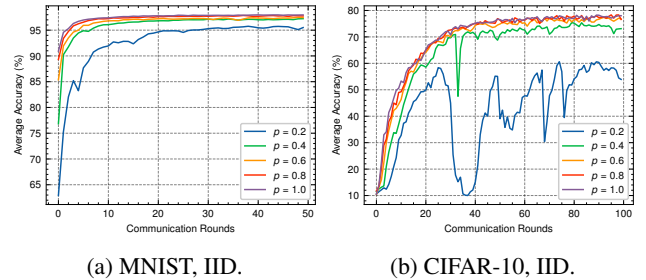


Figure 8: Effect of stragglers. The figures show the average accuracies of on-device models if only p portion of devices ($p \in \{0.2, 0.4, 0.6, 0.8, 1.0\}$) are trained in each round.

vices ($p = 0.2$) participates in the training. Stragglers do not have a large impact on FedZKT as long as the majority of devices participate in the learning.

5 Conclusions

Given the widespread yet heterogeneous devices nowadays, this paper proposed a new federated learning framework, FedZKT, towards heterogeneous on-device models via zero-shot knowledge transfer. To enable broad participation especially from resource-constraint devices, FedZKT assigns resource-intensive and lightweight computation tasks to the server and devices, respectively. Contrary to certain prior research upon a public dataset or a pre-trained generator, the server performs a zero-shot knowledge distillation without data-dependency concern. Extensive experiments demonstrate the effectiveness and the robustness of FedZKT towards heterogeneous on-device models and challenging federated learning scenarios, such as non-iid data distribution and straggler effects.

References

- Ba, L. J.; and Caruana, R. 2013. Do deep nets really need to be deep? *arXiv preprint arXiv:1312.6184*.
- Buciluă, C.; Caruana, R.; and Niculescu-Mizil, A. 2006. Model compression. In *Proceedings of the 12th ACM SIGKDD international conference on Knowledge discovery and data mining*, 535–541.
- Cai, H.; Gan, C.; Wang, T.; Zhang, Z.; and Han, S. 2019. Once-for-all: Train one network and specialize it for efficient deployment. *arXiv preprint arXiv:1908.09791*.
- Chang, H.; Shejwalkar, V.; Shokri, R.; and Houmansadr, A. 2019. Cronus: Robust and heterogeneous collaborative learning with black-box knowledge transfer. *arXiv preprint arXiv:1912.11279*.
- Chen, H.-Y.; and Chao, W.-L. 2020. Feddistill: Making bayesian model ensemble applicable to federated learning. *arXiv e-prints*, arXiv–2009.
- Chen, X.; Zhu, G.; Zhang, L.; Fang, Y.; Guo, L.; and Chen, X. 2021. Age-Stratified COVID-19 Spread Analysis and Vaccination: A Multitype Random Network Approach. *IEEE Transactions on Network Science and Engineering*.
- Choi, Y.; Choi, J.; El-Khamy, M.; and Lee, J. 2020. Data-free network quantization with adversarial knowledge distillation. In *Proceedings of the IEEE/CVF Conference on Computer Vision and Pattern Recognition Workshops*, 710–711.
- Clanuwat, T.; Bober-Irizar, M.; Kitamoto, A.; Lamb, A.; Yamamoto, K.; and Ha, D. 2018. Deep Learning for Classical Japanese Literature.
- Diao, E.; Ding, J.; and Tarokh, V. 2020. HeteroFL: Computation and communication efficient federated learning for heterogeneous clients. *arXiv preprint arXiv:2010.01264*.
- Fang, G.; Song, J.; Shen, C.; Wang, X.; Chen, D.; and Song, M. 2019. Data-free adversarial distillation. *arXiv preprint arXiv:1912.11006*.
- Glorot, X.; and Bengio, Y. 2010. Understanding the difficulty of training deep feedforward neural networks. In *Proceedings of the thirteenth international conference on artificial intelligence and statistics*, 249–256. JMLR Workshop and Conference Proceedings.
- Guha, N.; Talwalkar, A.; and Smith, V. 2019. One-shot federated learning. *arXiv preprint arXiv:1902.11175*.
- He, C.; Annamaram, M.; and Avestimehr, S. 2020. Group Knowledge Transfer: Federated Learning of Large CNNs at the Edge. *Advances in Neural Information Processing Systems*, 33.
- He, K.; Zhang, X.; Ren, S.; and Sun, J. 2016. Deep residual learning for image recognition. In *Proceedings of the IEEE conference on computer vision and pattern recognition*, 770–778.
- Hinton, G.; Vinyals, O.; and Dean, J. 2015. Distilling the knowledge in a neural network. *arXiv preprint arXiv:1503.02531*.
- Itahara, S.; Nishio, T.; Koda, Y.; Morikura, M.; and Yamamoto, K. 2020. Distillation-based semi-supervised federated learning for communication-efficient collaborative training with non-iid private data. *arXiv preprint arXiv:2008.06180*.
- Jeong, E.; Oh, S.; Kim, H.; Park, J.; Bennis, M.; and Kim, S.-L. 2018. Communication-efficient on-device machine learning: Federated distillation and augmentation under non-iid private data. *arXiv preprint arXiv:1811.11479*.
- Krizhevsky, A.; et al. 2009. Learning multiple layers of features from tiny images.
- LeCun, Y.; Bottou, L.; Bengio, Y.; Haffner, P.; et al. 1998. Gradient-based learning applied to document recognition. *Proceedings of the IEEE*, 86(11): 2278–2324.
- Li, D.; and Wang, J. 2019. Fedmd: Heterogenous federated learning via model distillation. *arXiv preprint arXiv:1910.03581*.
- Li, Q.; Diao, Y.; Chen, Q.; and He, B. 2021a. Federated learning on non-iid data silos: An experimental study. *arXiv preprint arXiv:2102.02079*.
- Li, T.; Sahu, A. K.; Talwalkar, A.; and Smith, V. 2020. Federated learning: Challenges, methods, and future directions. *IEEE Signal Processing Magazine*, 37(3): 50–60.
- Li, T.; Sahu, A. K.; Zaheer, M.; Sanjabi, M.; Talwalkar, A.; and Smith, V. 2018. Federated optimization in heterogeneous networks. *arXiv preprint arXiv:1812.06127*.
- Li, X.; Huang, K.; Yang, W.; Wang, S.; and Zhang, Z. 2019. On the convergence of fedavg on non-iid data. *arXiv preprint arXiv:1907.02189*.
- Li, Y.; Zhou, W.; Wang, H.; Mi, H.; and Hospedales, T. M. 2021b. FedH2L: Federated Learning with Model and Statistical Heterogeneity. *arXiv preprint arXiv:2101.11296*.
- Lin, J.; Chen, W.-M.; Lin, Y.; Cohn, J.; Gan, C.; and Han, S. 2020a. Mccnet: Tiny deep learning on iot devices. *arXiv preprint arXiv:2007.10319*.
- Lin, T.; Kong, L.; Stich, S. U.; and Jaggi, M. 2020b. Ensemble distillation for robust model fusion in federated learning. *arXiv preprint arXiv:2006.07242*.
- Liu, W.; Chen, L.; Chen, Y.; and Zhang, W. 2020. Accelerating federated learning via momentum gradient descent. *IEEE Transactions on Parallel and Distributed Systems*, 31(8): 1754–1766.
- Ma, N.; Zhang, X.; Zheng, H.-T.; and Sun, J. 2018. Shufflenet v2: Practical guidelines for efficient cnn architecture design. In *Proceedings of the European conference on computer vision (ECCV)*, 116–131.
- McMahan, B.; Moore, E.; Ramage, D.; Hampson, S.; and y Arcas, B. A. 2017. Communication-Efficient Learning of Deep Networks from Decentralized Data. In *Artificial Intelligence and Statistics*, 1273–1282.
- Micaelli, P.; and Storkey, A. 2019. Zero-shot knowledge transfer via adversarial belief matching. *arXiv preprint arXiv:1905.09768*.
- Nishio, T.; and Yonetani, R. 2019. Client selection for federated learning with heterogeneous resources in mobile edge. In *ICC 2019-2019 IEEE International Conference on Communications (ICC)*, 1–7. IEEE.
- Sandler, M.; Howard, A.; Zhu, M.; Zhmoginov, A.; and Chen, L.-C. 2018. Mobilenetv2: Inverted residuals and linear bottlenecks. In *Proceedings of the IEEE conference on computer vision and pattern recognition*, 4510–4520.

- Sattler, F.; Korjakow, T.; Rischke, R.; and Samek, W. 2021. FedAUX: Leveraging Unlabeled Auxiliary Data in Federated Learning. *arXiv preprint arXiv:2102.02514*.
- Sattler, F.; Marban, A.; Rischke, R.; and Samek, W. 2020. Communication-efficient federated distillation. *arXiv preprint arXiv:2012.00632*.
- Seo, H.; Park, J.; Oh, S.; Bennis, M.; and Kim, S.-L. 2020. Federated knowledge distillation. *arXiv preprint arXiv:2011.02367*.
- Sun, L.; and Lyu, L. 2020. Federated model distillation with noise-free differential privacy. *arXiv preprint arXiv:2009.05537*.
- Truong, J.-B.; Maini, P.; Walls, R. J.; and Papernot, N. 2021. Data-free model extraction. In *Proceedings of the IEEE/CVF Conference on Computer Vision and Pattern Recognition*, 4771–4780.
- Vepakomma, P.; Gupta, O.; Swedish, T.; and Raskar, R. 2018. Split learning for health: Distributed deep learning without sharing raw patient data. *arXiv preprint arXiv:1812.00564*.
- Wang, J.; Liu, Q.; Liang, H.; Joshi, G.; and Poor, H. V. 2020. Tackling the Objective Inconsistency Problem in Heterogeneous Federated Optimization. *Advances in Neural Information Processing Systems*, 33.
- Xiao, H.; Rasul, K.; and Vollgraf, R. 2017. Fashion-MNIST: a Novel Image Dataset for Benchmarking Machine Learning Algorithms.
- Yang, Q.; Liu, Y.; Chen, T.; and Tong, Y. 2019. Federated machine learning: Concept and applications. *ACM Transactions on Intelligent Systems and Technology (TIST)*, 10(2): 1–19.
- Zhu, Z.; Hong, J.; and Zhou, J. 2021. Data-Free Knowledge Distillation for Heterogeneous Federated Learning. *arXiv preprint arXiv:2105.10056*.

A Evaluation Details

In this section, we describe the details of evaluation setup and results.

A.1 Model Architecture

For the MNIST, KMNIST, and Fashion-MNIST datasets, we use five different model architectures as shown in Table 4 and adopt these architectures to the on-device models.

| Model A | | Model B | | Model C | |
|-----------------|------------------------|-----------------|-----------------------------------|-----------------|-----------------------------------|
| Layer Type | Parameter | Layer Type | Parameter | Layer Type | Parameter |
| Input Layer | | Input Layer | | Input Layer | |
| Convolution | 6 filters, kernel 5x5 | Convolution | 6 filters, kernel 5x5 | Convolution | 6 filters, kernel 5x5 |
| ReLU | | ReLU | | ReLU | |
| MaxPooling | kernel 5x5 | MaxPooling | kernel 5x5 | MaxPooling | kernel 5x5 |
| Convolution | 16 filters, kernel 5x5 | Convolution | 16 filters, kernel 5x5 | Convolution | 16 filters, kernel 5x5 |
| ReLU | | ReLU | | ReLU | |
| MaxPooling | kernel 5x5 | MaxPooling | kernel 5x5 | MaxPooling | kernel 5x5 |
| Fully Connected | 256 | Convolution | 16 filters, kernel 3x3, padding 1 | Convolution | 16 filters, kernel 3x3, padding 1 |
| ReLU | | ReLU | | ReLU | |
| Fully Connected | 84 | Fully Connected | 256 | Convolution | 16 filters, kernel 3x3, padding 1 |
| ReLU | | ReLU | | ReLU | |
| Fully Connected | 10 | Fully Connected | 84 | Fully Connected | 256 |
| | | ReLU | | ReLU | |
| | | Fully Connected | 10 | Fully Connected | 84 |
| | | | | ReLU | |
| | | | | Fully Connected | 10 |

| Model D | | Model E | |
|-----------------|-----------------------------------|-----------------|-----------|
| Layer Type | Parameter | Layer Type | Parameter |
| Input Layer | | Input Layer | |
| Convolution | 32 filters, kernel 3x3, padding 1 | Fully Connected | 128 |
| ReLU | | ReLU | |
| Convolution | 32 filters, kernel 3x3, padding 1 | Fully Connected | 64 |
| ReLU | | ReLU | |
| MaxPooling | kernel 2x2 | Fully Connected | 10 |
| Fully Connected | 64 | | |
| ReLU | | | |
| Fully Connected | 10 | | |

Table 4: Model Architecture used for the MNIST, KMNIST, FASHION datasets.

| Model A | | Model B | | Model C | | Model D | | Model E |
|--------------|--------------|--------------|--------------|-------------|----------------------|-------------|----------------------|---------|
| Arch | Parameter | Arch | Parameter | Arch | Parameter | Arch | Parameter | Arch |
| ShuffleNetV2 | net size 0.5 | ShuffleNetV2 | net size 1.0 | MobileNetV2 | width multiplier 0.8 | MobileNetV2 | width multiplier 0.6 | LeNet |

Table 5: Model Architecture for the CIFAR-10 dataset.

For the CIFAR-10 dataset, we use ShuffleNetV2 and MobileNetV2 with different numbers of filters and a LeNet-like model architectures to meet diverse device capacity for on-device models². Table 5 presents the detailed model architectures.

A.2 On-device Model Performance

We evaluate the performance of FedZKT on four datasets. In the main paper, we present the average accuracies of on-device models. Here, we present the accuracies of each on-device model in Table 6.

A.3 Lower and Upper Bounds of Model Performance

To evaluate the performance of FedZKT, we present the lower bound and upper bound of model architectures in Table 7. We consider the lower bound of model performance as the model trained on the on-device data only. To calculate the upper bound of model performance, we assume the on-device model can access all the local data. Therefore, the upper bound of model performance is the accuracy of the model trained on the all local data. To train the model with diverse architectures, we use SGD with a

²we implement the models based on <https://github.com/kuangliu/pytorch-cifar>.

| Device | Model Arch | On-device Accuracy | | | |
|-----------|------------|--------------------|---------|--------|----------|
| | | MNIST | FASHION | KMNIST | CIFAR-10 |
| Device 1 | Model A | 97.98% | 83.32% | 87.02% | 81.74% |
| Device 2 | Model B | 98.03% | 83.65% | 86.39% | 82.24% |
| Device 3 | Model C | 98.04% | 83.61% | 83.57% | 82.45% |
| Device 4 | Model D | 97.75% | 84.20% | 86.82% | 82.67% |
| Device 5 | Model E | 97.30% | 85.28% | 87.97% | 61.88% |
| Device 6 | Model A | 97.88% | 86.32% | 86.82% | 80.68% |
| Device 7 | Model B | 98.01% | 83.78% | 84.21% | 81.94% |
| Device 8 | Model C | 97.93% | 84.65% | 87.36% | 81.92% |
| Device 9 | Model D | 97.66% | 85.13% | 86.65% | 82.49% |
| Device 10 | Model E | 97.00% | 84.30% | 87.50% | 62.21% |

Table 6: On-device model accuracies using FedZKT on four datasets.

learning rate 0.01 and a weight decay of 0.0005. We set the batch size as 256 and the total training epochs as 50 for the MNIST dataset and 100 for the CIFAR-10 dataset.

| Device | Model Arch | MNIST | | CIFAR-10 | |
|-----------|------------|-------------|-------------|-------------|-------------|
| | | upper bound | lower bound | upper bound | lower bound |
| Device 1 | Model A | 99.12% | 97.58% | 84.18% | 50.17% |
| Device 2 | Model B | 99.16% | 97.29% | 86.98% | 54.08% |
| Device 3 | Model C | 99.06% | 97.21% | 88.63% | 58.56% |
| Device 4 | Model D | 98.88% | 96.98% | 87.36% | 57.84% |
| Device 5 | Model E | 98.07% | 94.43% | 70.77% | 58.90% |
| Device 6 | Model A | 98.87% | 97.26% | 84.39% | 50.13% |
| Device 7 | Model B | 99.23% | 96.93% | 85.99% | 51.07% |
| Device 8 | Model C | 99.08% | 97.16% | 88.34% | 62.15% |
| Device 9 | Model D | 98.85% | 96.78% | 88.87% | 59.88% |
| Device 10 | Model E | 97.99% | 94.24% | 70.65% | 54.81% |

Table 7: Lower and Upper Bound of Model Performance.

B Choice of The Loss Function

This section justifies the Hypothesis 1 and 2 for choosing the loss function in Algorithm 3 (Eq. 2).

Given the global model \mathcal{F} , on-device models f_k $k \in \mathcal{K}$, input data x , we define the outputs of global model after the softmax layer as $U = \mathcal{F}(x)$ and the logit outputs of the on-device models as $V_k = f_k(x)$. Therefore, the logit output before softmax layer are u and v_k for the global and on-device models, respectively. We have $U = \text{softmax}(u)$ and $V_k = \text{softmax}(v_k)$.

B.1 ℓ_1 norm loss

The ℓ_1 norm loss is defined as:

$$\mathcal{L}_{\ell_1} = \|u - \frac{1}{|\mathcal{K}|} \sum_k v_k\|_1. \quad (10)$$

The gradients of ℓ_1 norm loss with respect to input x are:

$$\nabla_x \mathcal{L}_{\ell_1} = \sum_i \text{sign}(u^i - \frac{1}{|\mathcal{K}|} \sum_j v_j^i) \left(\frac{\partial u^i}{\partial x} - \frac{\partial (\frac{1}{|\mathcal{K}|} \sum_k v_k^i)}{\partial x} \right), \quad (11)$$

$$= \sum_i \text{sign}(u^i - \frac{1}{|\mathcal{K}|} \sum_j v_j^i) \frac{1}{|\mathcal{K}|} \sum_k \left(\frac{\partial u^i}{\partial x} - \frac{\partial v_k^i}{\partial x} \right), \quad (12)$$

$$= \frac{1}{|\mathcal{K}|} \sum_i \sum_k \text{sign}(u^i - \frac{1}{|\mathcal{K}|} \sum_j v_j^i) \left(\frac{\partial u^i}{\partial x} - \frac{\partial v_k^i}{\partial x} \right), \quad (13)$$

where i denotes the dimension of output. Then the norm of gradients of ℓ_1 norm loss can be written as:

$$\|\nabla_x \mathcal{L}_{\ell_1}\| = \frac{1}{|\mathcal{K}|} \left\| \sum_i \sum_k \text{sign}(u^i - \frac{1}{|\mathcal{K}|} \sum_k v_k^i) (\frac{\partial u^i}{\partial x} - \frac{\partial v_k^i}{\partial x}) \right\|. \quad (14)$$

B.2 KL divergence loss

The KL divergence loss is defined as:

$$\mathcal{L}_{\text{KL}} = \sum_i U^i \log \frac{U^i}{\frac{1}{|\mathcal{K}|} \sum_k V_k^i}. \quad (15)$$

The gradients of KL-divergence loss with respect to input x is:

$$\nabla_x \mathcal{L}_{\text{KL}} = \sum_i \frac{\partial U^i}{\partial x} \log \frac{U^i}{\frac{1}{|\mathcal{K}|} \sum_k V_k^i} - \frac{\partial(\frac{1}{|\mathcal{K}|} \sum_k V_k^i)}{\partial x} \frac{U^i}{\frac{1}{|\mathcal{K}|} \sum_k V_k^i}. \quad (16)$$

When U converges to the ensemble of V_k , then

$$U(x) = \frac{1}{|\mathcal{K}|} \sum_k V_k(x)(1 + \delta(x)), \quad (17)$$

where $\delta(x) \xrightarrow{F \rightarrow f_{\text{ens}}} 0$. Therefore, the gradients of KL divergence loss (Eq. 17) become:

$$\begin{aligned} \nabla_x \mathcal{L}_{\text{KL}} &\approx \sum_i \frac{\partial U^i}{\partial x} \delta_i - \frac{\partial(\frac{1}{|\mathcal{K}|} \sum_k V_k^i)}{\partial x} (1 + \delta_i) \quad (\text{since } \log(1 + \delta) \xrightarrow{\delta \rightarrow 0} \delta) \\ &= \sum_i \delta_i \left(\frac{\partial U^i}{\partial x} - \frac{\partial(\frac{1}{|\mathcal{K}|} \sum_k V_k^i)}{\partial x} \right) \quad (\forall k, \sum_i \frac{\partial V_k^i}{\partial x} = 0, \text{ since } \sum_i V_k^i = 1), \\ &= \frac{1}{|\mathcal{K}|} \sum_i \sum_k \delta_i \left(\frac{\partial U^i}{\partial x} - \frac{\partial V_k^i}{\partial x} \right) \end{aligned} \quad (18)$$

The norm of the gradients of KL-divergence loss can be written as:

$$\|\nabla_x \mathcal{L}_{\text{KL}}\| \approx \frac{1}{|\mathcal{K}|} \left\| \sum_i \sum_k \delta_i \left(\frac{\partial U^i}{\partial x} - \frac{\partial V_k^i}{\partial x} \right) \right\|. \quad (19)$$

B.3 SL Loss

The proposed SL loss is defined as:

$$\mathcal{L}_{\text{SL}} = \|U - \frac{1}{|\mathcal{K}|} \sum_k V_k\|_1. \quad (20)$$

Similarly to the ℓ_1 norm loss, the gradients of SL loss with respect to input x are:

$$\nabla_x \mathcal{L}_{\text{SL}} = \frac{1}{|\mathcal{K}|} \sum_i \sum_k \text{sign}(U^i - \frac{1}{|\mathcal{K}|} \sum_j V_j^i) \left(\frac{\partial U^i}{\partial x} - \frac{\partial V_k^i}{\partial x} \right). \quad (21)$$

The norm of gradients of SL loss can be written as:

$$\|\nabla_x \mathcal{L}_{\text{SL}}\| = \frac{1}{|\mathcal{K}|} \left\| \sum_i \sum_k \text{sign}(U^i - \frac{1}{|\mathcal{K}|} \sum_j V_j^i) \left(\frac{\partial U^i}{\partial x} - \frac{\partial V_k^i}{\partial x} \right) \right\|. \quad (22)$$

B.4 Justification of Two Hypotheses

We introduce two lemmas provided in (Truong et al. 2021).

Lemma 1. *Let J be the Jacobian matrix of softmax function, then for any vector z , we have:*

$$\forall z, \quad \|Jz\| \leq \|z\|. \quad (23)$$

Lemma 2. *Let $U(x)$ and $V(x)$ be the softmax output of differential functions on input x , with respective logits $u(x)$ and $v(x)$. When U converges to V then $\frac{\partial U}{\partial u}$ converges to $\frac{\partial V}{\partial v}$.*

Then we provide justification of Hypothesis 1 and 2. Following the proof provided in (Truong et al. 2021), we provide justification for the proposed SL loss in federated learning.

Proof. For ℓ_1 norm loss, each term in the norm of gradients (Eq. 14) is:

$$\forall i, k \quad \left\| \text{sign}\left(u^i - \frac{1}{|\mathcal{K}|} \sum_j v_j^i\right) \left(\frac{\partial u^i}{\partial x} - \frac{\partial v_k^i}{\partial x} \right) \right\| = \left\| \frac{\partial u^i}{\partial x} - \frac{\partial v_k^i}{\partial x} \right\| \quad (24)$$

For SL loss, when the global model converges to the ensemble of on-device models, each term in the norm of gradients (Eq. 22) is:

$$\begin{aligned} \forall i, k \quad \left\| \text{sign}\left(U^i - \frac{1}{|\mathcal{K}|} \sum_j V_j^i\right) \left(\frac{\partial U^i}{\partial x} - \frac{\partial V_k^i}{\partial x} \right) \right\| &= \left\| \frac{\partial U^i}{\partial x} - \frac{\partial V_k^i}{\partial x} \right\| \quad (25) \\ &= \left\| \frac{\partial U^i}{\partial u} \frac{\partial u^i}{\partial x} - \frac{\partial V_k^i}{\partial v} \frac{\partial v_k^i}{\partial x} \right\|, \\ &\approx \left\| \frac{\partial U^i}{\partial u} \left(\frac{\partial u^i}{\partial x} - \frac{\partial v_k^i}{\partial x} \right) \right\| \quad (\text{Lemma 2}), \\ &\leq \left\| \frac{\partial u^i}{\partial x} - \frac{\partial v_k^i}{\partial x} \right\| \quad (\text{Lemma 1}). \quad (26) \end{aligned}$$

Therefore, summing up the terms over i and k , we expect the gradients of SL loss is smaller than the ℓ_1 norm loss (Hypothesis 2). However, to rigorously proof this, we need further assumptions on the data distribution and models.

For KL loss, when the global model converges to the ensemble of on-device models, each term in the norm of gradients (Eq. 18) can be written as:

$$\forall i, k \quad \left\| \delta_i \left(\frac{\partial U^i}{\partial x} - \frac{\partial V_k^i}{\partial x} \right) \right\|. \quad (27)$$

Comparing Eq. 25 and 27, we expect the gradient of KL divergence loss is smaller than that of the SL loss (Hypothesis 1). \square